

# Observing and modeling the extragalactic ISM

Vianney Lebouteiller (CNRS/AIM, CEA Saclay)

# Outline

- **External galaxies**
  - Parameter space
  - The ISM within the galaxy evolution and star formation contexts
- **Some highlights**
- **Modeling strategies**
  - Accounting for the ISM complexity & structure

*(Wide topic, focus on spectroscopy and gas tracers)*

# Physical scales & components

Physical processes generally act on / originate from a wide range of spatial scales (e.g., SF)

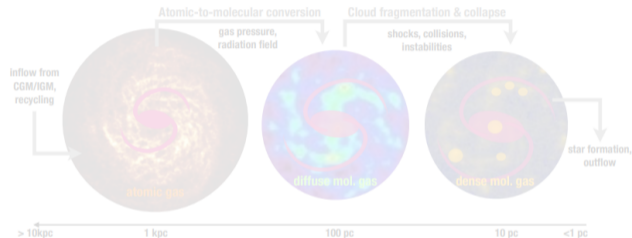


Fig.: HI-H<sub>2</sub> conversion and SF process as a function of spatial scales (Saintonge+ 2022).

## Main challenges for extragalactic observations

- Reach small enough scales to disentangle ISM components or recover them through indirect, integrated, signatures
- Understand/generalize physical mechanisms in conditions  $\neq$  from MW

# Physical scales & components

Physical processes generally act on / originate from a wide range of spatial scales (e.g., SF)

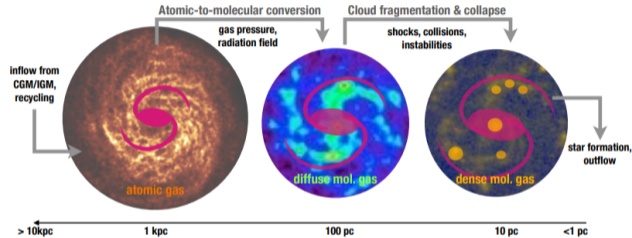


Fig.: HI-H<sub>2</sub> conversion and SF process as a function of spatial scales (Saintonge+ 2022).

## Main challenges for extragalactic observations

- Reach small enough scales to disentangle ISM components or recover them through indirect, integrated, signatures
- Understand/generalize physical mechanisms in conditions  $\neq$  from MW

# Physical scales & components

Physical processes generally act on / originate from a wide range of spatial scales (e.g., SF)

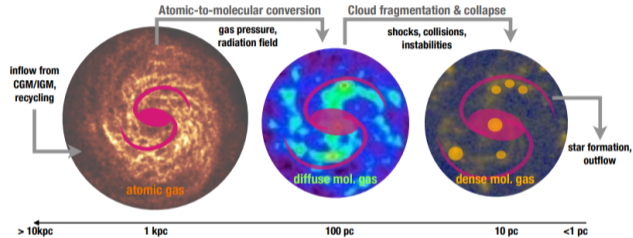


Fig.: HI-H<sub>2</sub> conversion and SF process as a function of spatial scales (Saintonge+ 2022).

## Main challenges for extragalactic observations

- Reach small enough scales to disentangle **ISM components** or recover them through indirect, integrated, signatures
- Understand/generalize **physical mechanisms** in conditions  $\neq$  from MW

# Physical scales & components

Digest & process wealth of spatial information

Combine detailed ISM models with state-of-the-art radiative transfer and chemistry + complex enough geometries



*Fig.: NGC 4254, MUSE (blue/yellow) + ALMA (orange), PHANGS*



*Fig.: NGC 7496, HST+JWST, PHANGS*

# Expanding the parameter space and generalizing mechanisms

## Detailed studies of nearby galaxies. . .

- $\neq$  environments at large
  - Z & ISM phases, young stellar clusters, X-ray binaries, AGNs, interactions. . .
- $\neq$  predominance of physical processes
  - Photoelectric effect, X-ray photoionization, CR ionization, shocks. . .
- **Main obstacles**
  - Knowledge of dust & energetic sources
  - Mixing biases when dealing with poor/no spatial/spectral resolution

## . . . to be adapted to the Early Universe

- Multiphase ISM also revealed at very high-z (e.g., (CII)  $158 \mu\text{m}$ , (OIII)  $88 \mu\text{m}$  (e.g., *Harikane+ 2020*)
- Spatial information increasingly available (e.g., *Wong+ 2022, Dye+ 2022*)

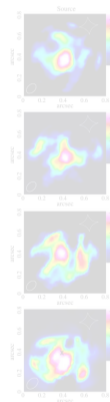


Fig.: CO(7-6),  $\text{H}_2$ , and (C I) lines in a  $z = 4.24$  lensed galaxy with ALMA (*Dye+ 2022*)

# Expanding the parameter space and generalizing mechanisms

## Detailed studies of nearby galaxies. . .

- $\neq$  environments at large
  - Z & ISM phases, young stellar clusters, X-ray binaries, AGNs, interactions. . .
- $\neq$  predominance of physical processes
  - Photoelectric effect, X-ray photoionization, CR ionization, shocks. . .
- **Main obstacles**
  - Knowledge of dust & energetic sources
- Mixing biases when dealing with poor/no spatial/spectral resolution

## . . . to be adapted to the Early Universe

- Multiphase ISM also revealed at very high-z (e.g., (CII) 158  $\mu\text{m}$ , (OIII) 88  $\mu\text{m}$  (e.g., *Harikane+ 2020*)
- Spatial information increasingly available (e.g., *Wong+ 2022, Dye+ 2022*)

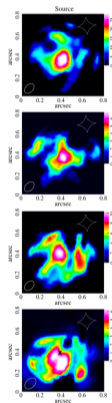


**Fig.:** CO(7-6), H<sub>2</sub>, and (C I) lines in a  $z = 4.24$  lensed galaxy with ALMA (*Dye+ 2022*)



## Cosmic noon zoom

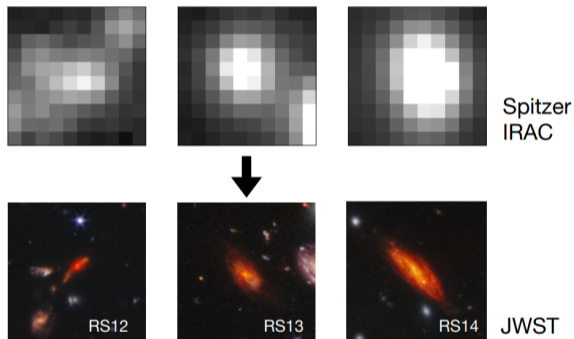


*Fig.: IRAC1 blobs in SMACS0723 field are likely  $z=1-3$  red spiral galaxies (NIRcam; Fudamoto+ 2022)*

... but spectra of  $z \gtrsim 3$  galaxies will remain spatially-unresolved with JWST for the most part

# Exploring the metal-poor ISM

- Mass-metallicity relation (MZR): **metal-enriched outflow** rate, variable integrated IMF, infall (radial for low  $M^*$  vs. cosmological for high  $M^*$ ) rate (e.g., Spitoni+ 2010)

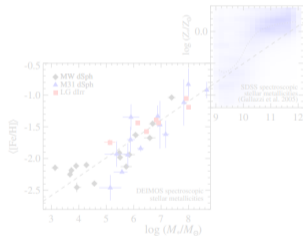
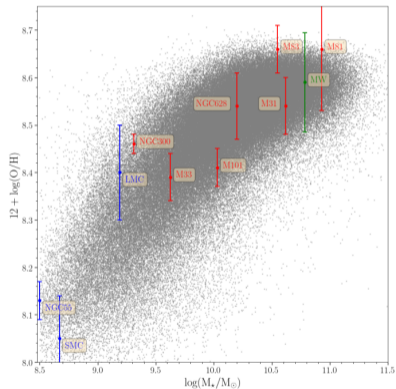


Fig.: MZR in Local Group dIrr and dSph (Kirby+ 2013)

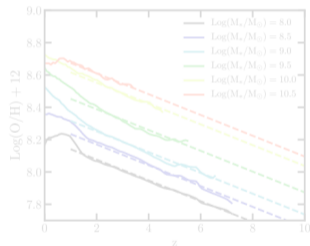


Fig.: MZR vs.  $z$  in cosmological simulations (IllustrisTNG; Torrey+ 2019). Absolute calibration somewhat uncertain due to  $Z$  calibration with observations.

Fig.: MZR in the local Universe and SDSS  $z < 0.2$  galaxies (Duarte Puertas+ 2022)

# Exploring the metal-poor ISM

- Mass-metallicity relation (MZR): **metal-enriched outflow** rate, variable integrated IMF, infall (radial for low  $M^*$  vs. cosmological for high  $M^*$ ) rate (e.g., Spitoni+ 2010)

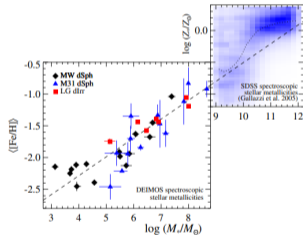
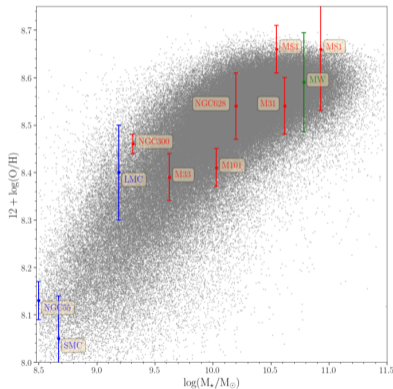


Fig.: MZR in Local Group dIrr and dSph (Kirby+ 2013)

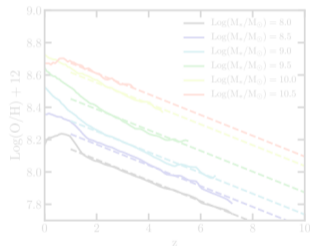


Fig.: MZR vs.  $z$  in cosmological simulations (IllustrisTNG; Torrey+ 2019). Absolute calibration somewhat uncertain due to  $Z$  calibration with observations.

Fig.: MZR in the local Universe and SDSS  $z < 0.2$  galaxies (Duarte Puertas+ 2022)

# Exploring the metal-poor ISM

- Mass-metallicity relation (MZR): **metal-enriched outflow** rate, variable integrated IMF, infall (radial for low  $M^*$  vs. cosmological for high  $M^*$ ) rate (e.g., Spitoni+ 2010)

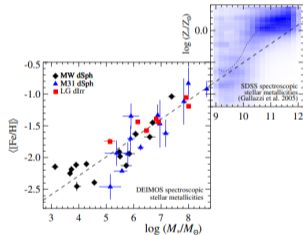
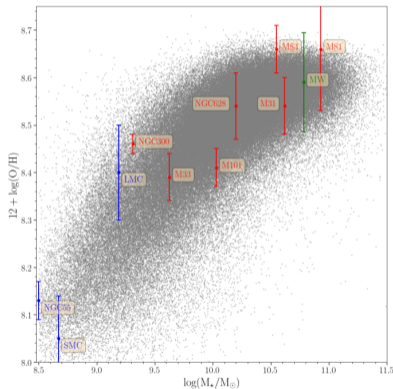


Fig.: MZR in Local Group dIrr and dSph (Kirby+ 2013)

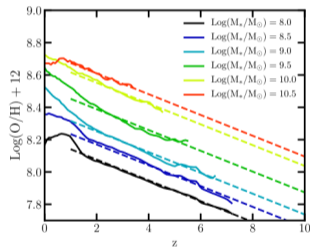
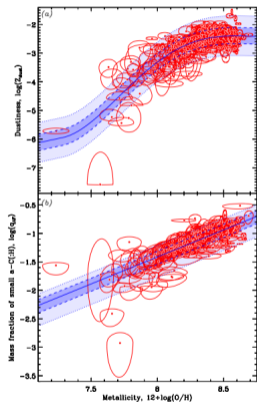


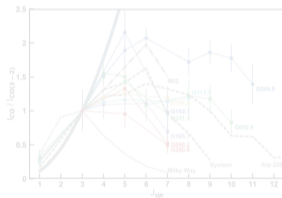
Fig.: MZR vs.  $z$  in cosmological simulations (IllustrisTNG; Torrey+ 2019). Absolute calibration somewhat uncertain due to  $Z$  calibration with observations.

Fig.: MZR in the local Universe and SDSS  $z < 0.2$  galaxies (Duarte Puertas+ 2022)

# Observed diversity in the ISM composition/physical conditions



**Fig.:** D/G and mass fraction of small amorphous carbons (Galliano+ 2021)



**Fig.:** CO SLED (Cañameras+ 2018)

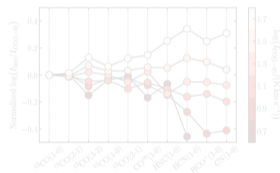


**Fig.:** Molecular line ratios in M51 (CLAWS: den Brok+ 2022)

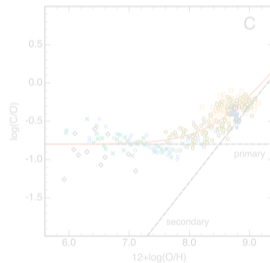


**Fig.:** C/O gas phase abundance ratio (Nicholls+ 2017)

# Observed diversity in the ISM composition/physical conditions

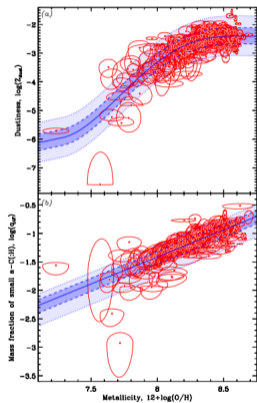


Fig.: D/G and mass fraction of small amorphous carbons (Galliano+ 2021)

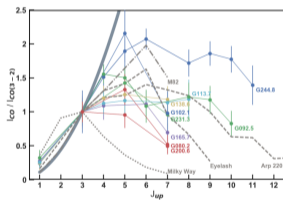


Fig.: CO SLED (Cañameras+ 2018)

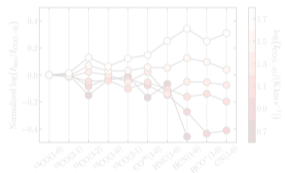


Fig.: Molecular line ratios in M51 (CLAWS: den Brok+ 2022)

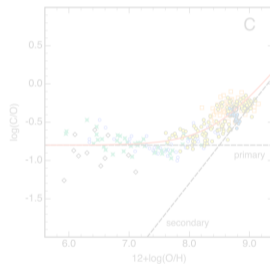


Fig.: C/O gas phase abundance ratio (Nicholls+ 2017)

# Observed diversity in the ISM composition/physical conditions

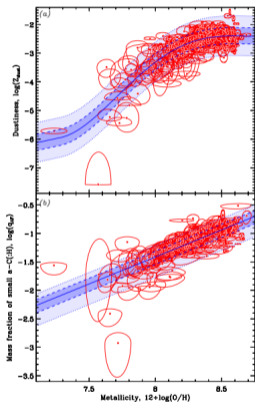


Fig.: D/G and mass fraction of small amorphous carbons (Galliano+ 2021)

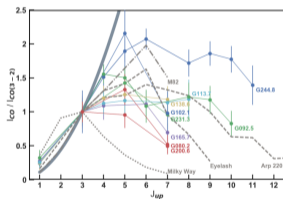


Fig.: CO SLED (Cañameras+ 2018)

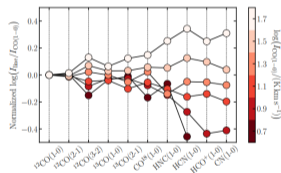


Fig.: Molecular line ratios in M51 (CLAWS; den Brok+ 2022)

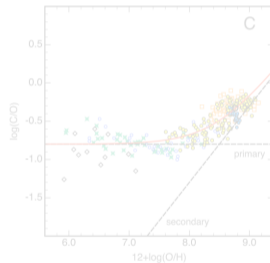


Fig.: C/O gas phase abundance ratio (Nicholls+ 2017)

# Observed diversity in the ISM composition/physical conditions

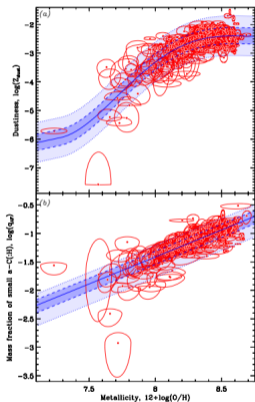


Fig.: D/G and mass fraction of small amorphous carbons (Galliano+ 2021)

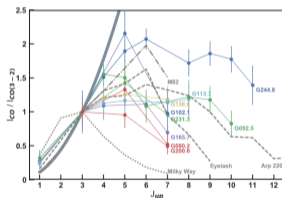


Fig.: CO SLED (Cañameras+ 2018)

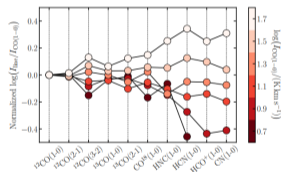


Fig.: Molecular line ratios in M51 (CLAWS; den Brok+ 2022)

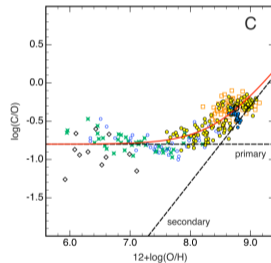


Fig.: C/O gas phase abundance ratio (Nicholls+ 2017)



# Observed diversity in the radiation sources

## Young massive clusters

- Upper cut-off mass value debated (Mok+2019) but maximum L & M reach  $\gtrsim 2$  dex above MW (Portegies Zwart 2010)

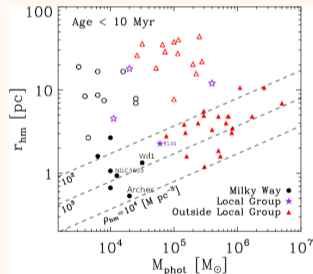


Fig.: Mass-size relationship in young star clusters and associations (Portegies Zwart 2010, Santoro+ 2022)

## High-mass X-ray binaries

- Often dominate the high-E output from nearby actively SF galaxies (e.g. Grimm+2003, Mineo+2012)
- Typically provide  $\sim 10^{39-41}$  erg/s (i.e.,  $\sim 1-10\%$  of total L!). Feedback may keep the (dust-poor) ISM warm without removing a significant gas fraction (Artale+2015)
- Higher abundance & luminosity at low Z / high z (Gilbertson+2022, Lehmer+2021)
- Mass of stellar accreting partner & SFR correlation hints at production site / presence in young massive clusters

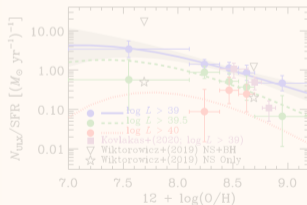


Fig.: Number of ULXs per unit SFR as a function of metallicity (Lehmer+ 2021).

# Observed diversity in the radiation sources

## Young massive clusters

- Upper cut-off mass value debated (Mok+2019) but maximum L & M reach  $\gtrsim 2$  dex above MW (Portegies Zwart 2010)

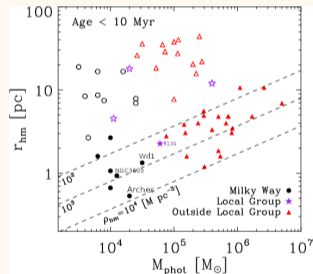


Fig.: Mass-size relationship in young star clusters and associations (Portegies Zwart 2010, Santoro+ 2022)

## High-mass X-ray binaries

- Often dominate the high-E output from nearby actively SF galaxies (e.g. Grimm+2003, Mineo+ 2012)
- Typically provide  $\sim 10^{39-41}$  erg/s (i.e.,  $\sim 1-10\%$  of total L!). Feedback may keep the (dust-poor) ISM warm without removing a significant gas fraction (Artale+ 2015)
- Higher abundance & luminosity at low Z / high z (Gilbertson+ 2022, Lehmer+ 2021)
- Mass of stellar accreting partner & SFR correlation hints at production site / presence in young massive clusters

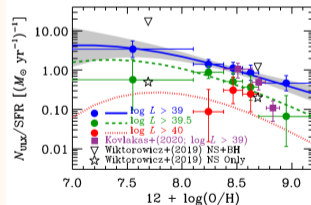


Fig.: Number of ULXs per unit SFR as a function of metallicity (Lehmer+ 2021).

# Cold ISM within the galaxy evolution context

Star-formation main sequence (MS; SFR vs.  $M_*$ ) set by gas content and efficiency gas  $\rightarrow$  stars

- MS **normalization** with  $z$  set by available gas supply from accretion
- At low  $z$ , **position along MS**, including flattening above  $M_{knee}$ , follows  $M_{H_2}$  vs.  $M_*$  while **scatter around MS** follows molecular gas fraction
- Time-independent shape of MS  $\Rightarrow$  long SF duty cycles ( $\sim$  Gyr) as opposed to quick  $\uparrow\downarrow$  due to SFH) (e.g., *Saintonge+ 2022*)
- Strong function of  $M_*$ : low mass galaxies in particular have extended HI reservoirs largely decoupled from the star formation process.
- Equilibrium of gas accretion, star formation, and gas outflows : the "gas regulator models" (e.g., *Bouché+10; Davé+12; Rathaus+16; Tacchella+20*)

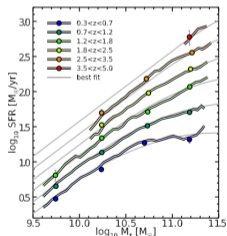


Fig.: MS vs.  $z$  with Herschel stacking (Schreiber+ 2014)

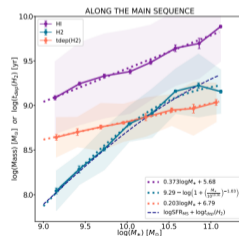
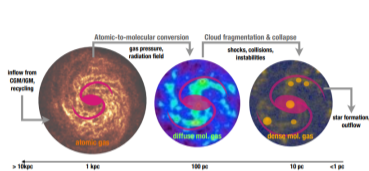


Fig.: Mass relationships (Saintonge+ 2022)

# Cold ISM within the SF context



## Dense gas fraction

- SF set by processes acting on different spatial scales
  - CO does not trace well the dense molecular gas (e.g., Roman-Duval+ 2016)
- Accounting for dense gas fraction within galaxies still results in non-constant SFE (EMPIRE: Jiménez-Donaire+ 2019, Besic+ 2021)
  - Dense gas threshold SF models (universal  $\tau_{\text{dep}}$  above  $n_T$ ) may remain valid at small scales (<100pc)  $\Rightarrow$  use tracers with even higher critical densities?
  - Turbulence-regulated SF models with feedback (e.g., Krumholz & Mc Kee 2005, Federath & Klessen 2012)?

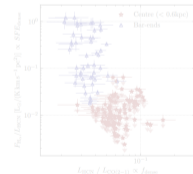
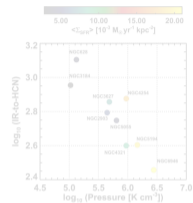
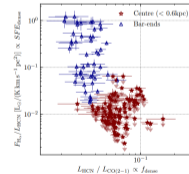
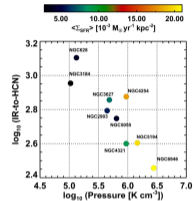
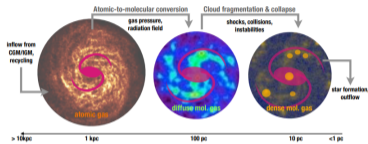


Fig.: Top: SFE(dense) vs.  $P$  in EMPIRE (Jiménez-Donaire+ 2019), bottom: vs.  $f(\text{dense})$  in NGC3627 (Besic+ 2021)

# Cold ISM within the SF context



**Fig.:** Top: SFE(dense) vs.  $P$  in EMPIRE (Jiménez-Donaire+ 2019), bottom: vs.  $f(\text{dense})$  in NGC3627 (Beslic+ 2021)

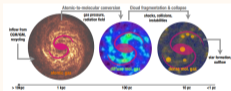
## Dense gas fraction

- SF set by processes acting on different spatial scales
  - CO does not trace well the dense molecular gas (e.g., Roman-Duval+ 2016)
- Accounting for dense gas fraction within galaxies still results in non-constant SFE (EMPIRE: Jiménez-Donaire+ 2019, Beslic+ 2021)
  - Dense gas threshold SF models (universal  $\tau_{\text{dep}}$  above  $n_{\text{t}}$ ) may remain valid even at small scales (<100pc)  $\Rightarrow$  use tracers with even higher critical densities?
  - Turbulence-regulated SF models with feedback (e.g., Krumholz & Mc Kee 2005, Federrath & Klessen 2012)?

# Physical processes to explore in a comprehensive way

## Gas & SF

- How do molecular clouds form, how long do they live? What sets the SFE?
- Conversion diffuse → dense, molecular gas vs. SF (CO-dark  $H_2$ , SK law)



- SF process itself  $\sim pc$ -scales: studies of protostars, SF filaments, and cloud-cloud collisions in Magellanic Clouds
- Hot cores and complex organic molecules in the LMC ( $CH_3OCH_3$ ,  $CH_3OCHO$ ... with ALMA), chemical differences may suggest local mixing of gas with  $\neq$  metallicity (Sewilo+ 2018, 2022)
- Protostellar CO outflows in the SMC with ALMA (Takuda+ 2022)
- More to come with JWST, ELT...

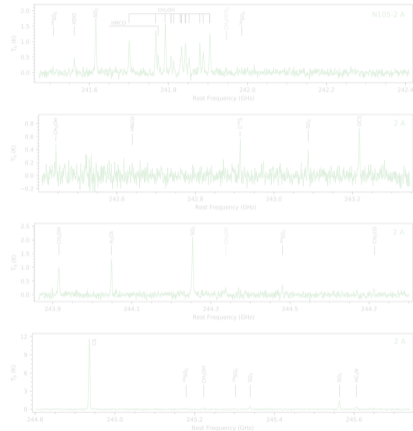
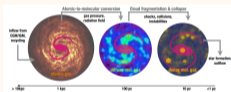


Fig.: Bona fide hot core in the LMC (Sewilo+ 2022)

# Physical processes to explore in a comprehensive way

## Gas & SF

- How do molecular clouds form, how long do they live? What sets the SFE?
- Conversion diffuse  $\rightarrow$  dense, molecular gas vs. SF (CO-dark  $H_2$ , SK law)



- SF process itself  $\sim$  pc-scales: studies of protostars, SF filaments, and cloud-cloud collisions in Magellanic Clouds
  - Hot cores and complex organic molecules in the LMC ( $CH_3OCH_3$ ,  $CH_3OCHO$ ... with ALMA), chemical differences may suggest local mixing of gas with  $\neq$  metallicity (Sewilo+ 2018, 2022)
  - Protostellar CO outflows in the SMC with ALMA (Tokuda+ 2022)
  - More to come with JWST, ELT...

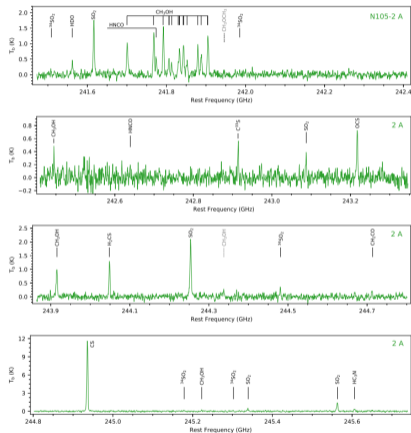


Fig.: Bona fide hot core in the LMC (Sewilo+ 2022)

# Physical processes to explore in a comprehensive way (cont'd)

## Turbulence

- $\text{CH}^+$  out-of-equilibrium  $\text{H}_2$  / dissipation of mechanical energy in turbulence (Godard+ 2022)
- At high-z: shock waves powered by hot galactic winds & turbulent cool gas reservoirs (e.g., Vidal-Garcia+ 2021, Falgarone+ 2017, Muller+ 2017) ⇒ **A. Vidal-Garcia's talk**

## Magnetic field

- SALSA Legacy Program: SOFIA HAWK+ observations of 14 nearby galaxies (Lopez-Rodriguez+ 2022)

Starburst ring of NGC 1097: B-field orientation and direction within 1 Kpc

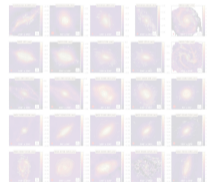
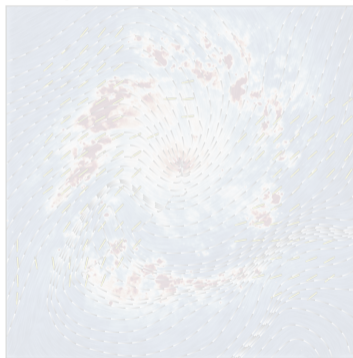


Fig.: SALSA NGC 1097 (Lopez-Rodriguez+ 2022)



# Physical processes to explore in a comprehensive way (cont'd)

## Turbulence

- $\text{CH}^+$  out-of-equilibrium  $\text{H}_2$  / dissipation of mechanical energy in turbulence (Godard+ 2022)
- At high-z: shock waves powered by hot galactic winds & turbulent cool gas reservoirs (e.g., Vidal-Garcia+ 2021, Falgarone+ 2017, Muller+ 2017)  $\Rightarrow$  **A. Vidal-Garcia's talk**

## Magnetic field

- SALSA Legacy Program: SOFIA HAWK+ observations of 14 nearby galaxies (Lopez-Rodriguez+ 2022)

Starburst ring of NGC 1097: B-field orientation and direction within 1 Kpc

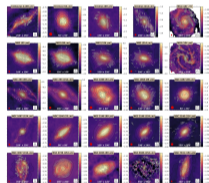
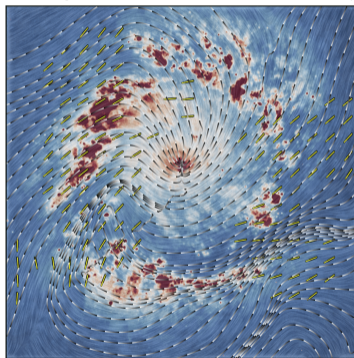


Fig.: SALSA NGC 1097 (Lopez-Rodriguez+ 2022)

# Some highlights

# CO-dark molecular gas and (CII)

⇒ S. Madden's talk

MW

- Dark gas mass fraction not traced by CO or HI is 20 – 40% in MW, most likely (CO-dark) molecular gas (DMG) as opposed to optically-thick HI (*Grenier+ 2005, Wolfire+ 2010, Hayashi+ 2019, Murray+ 2018*)

Local Group

- $f_{\text{DMG}} \approx 80\text{-}90\%$  in SMC/LMC SF regions (e.g., *Piñeda+ 2017, Lebauteiller+ 2019*)
- $\alpha_{\text{CO}} > \text{MW}$
- ... but fully accountable for by the CO filling factor (i.e., confirming that Z effect is to reduce the filling factor of molecular gas traced by CO due to low D/G) (*Piñeda+ 2017*) (see also *Mookerjee+ 2016 in M33*)

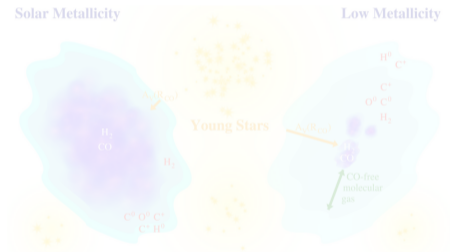


Fig.: (Madden+ 2020)

# CO-dark molecular gas and (CII)

⇒ S. Madden's talk

MW

- Dark gas mass fraction not traced by CO or HI is 20 – 40% in MW, most likely (CO-dark) molecular gas (DMG) as opposed to optically-thick HI (*Grenier+ 2005, Wolfire+ 2010, Hayashi+ 2019, Murray+ 2018*)

Local Group

- $f_{\text{DMG}} \approx 80\text{-}90\%$  in SMC/LMC SF regions (*e.g., Piñeda+ 2017, Lebouteiller+ 2019*)
- $\alpha_{\text{CO}} > \text{MW}$
- ... but fully accountable for by the CO filling factor (i.e., confirming that Z effect is to reduce the filling factor of molecular gas traced by CO due to low D/G) (*Piñeda+ 2017*) (*see also Mookerjee+ 2016 in M33*)

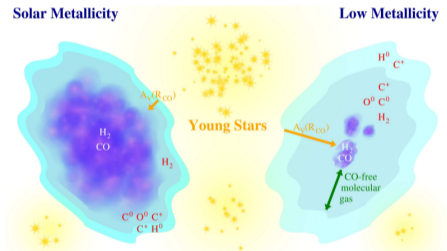


Fig.: (Madden+ 2020)

# CO-dark molecular gas and (CII) (cont'd)

## Extragalactic observations

- (CII) and other emission-lines readily available **at high-z**
- From models, (CII) and (CI) become increasingly good tracers of the  $H_2$  column density profile at low Z and for cosmic ray ionization rate  $\zeta_H \gtrsim 10^{-14} \text{ s}^{-1}$  (*Bisbas+ 2021*)
- **Dwarf Galaxy Survey** (metal-poor SF galaxies) (*Madden+ 2013*)
  - Integrated (CII) emission
  - $f_{\text{DMG}} \approx 70\text{-}100\%$ ,  $M_{\text{H}_2}$  follows closely  $L_{\text{CII}}$  in a single 1D model approach where  $A_V$  traced by (CII)/CO is the main parameter (*Madden+ 2020*)
  - CO-to- $H_2$  conversion factor ( $\alpha_{\text{CO}}$ ) not a simple function of Z but depends on the CO filling factor which can be partly recovered from the models (*Ramambason+ in prep.*)

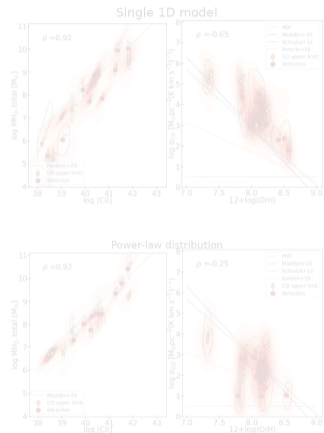


Fig.: CO-to- $H_2$  value between MW value and extreme case of CO uniformly distributed (*Ramambason+ in prep.*) ( $\Rightarrow$  L. Ramambason's poster)

# CO-dark molecular gas and (CII) (cont'd)

## Extragalactic observations

- (CII) and other emission-lines readily available **at high-z**
- From models, (CII) and (CI) become increasingly good tracers of the H<sub>2</sub> column density profile at low Z and for cosmic ray ionization rate  $\zeta_H \gtrsim 10^{-14} \text{ s}^{-1}$  (*Bisbas+ 2021*)
- **Dwarf Galaxy Survey** (metal-poor SF galaxies) (*Madden+ 2013*)
  - Integrated (CII) emission
  - $f_{\text{DMG}} \approx 70\text{-}100\%$ ,  $M_{\text{H}_2}$  follows closely  $L_{\text{CII}}$  in a single 1D model approach where  $A_V$  traced by (CII)/CO is the main parameter (*Madden+ 2020*)
  - CO-to-H<sub>2</sub> conversion factor ( $\alpha_{\text{CO}}$ ) not a simple function of Z but depends on the CO filling factor which can be partly recovered from the models (*Ramambason+ in prep.*)

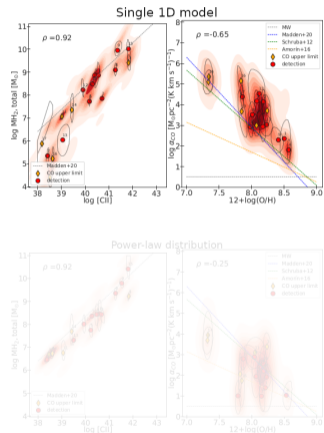


Fig.: CO-to-H<sub>2</sub> value between MW value and extreme case of CO uniformly distributed (*Ramambason+ in prep.*) ( $\Rightarrow$  L. Ramambason's poster)

# CO-dark molecular gas and (CII) (cont'd)

## Extragalactic observations

- (CII) and other emission-lines readily available **at high-z**
- From models, (CII) and (CI) become increasingly good tracers of the H<sub>2</sub> column density profile at low Z and for cosmic ray ionization rate  $\zeta_H \gtrsim 10^{-14} \text{ s}^{-1}$  (*Bisbas+ 2021*)
- **Dwarf Galaxy Survey** (metal-poor SF galaxies) (*Madden+ 2013*)
  - Integrated (CII) emission
  - $f_{\text{DMG}} \approx 70\text{-}100\%$ , M<sub>H2</sub> follows closely L<sub>CII</sub> in a single 1D model approach where A<sub>V</sub> traced by (CII)/CO is the main parameter (*Madden+ 2020*)
  - CO-to-H<sub>2</sub> conversion factor ( $\alpha_{\text{CO}}$ ) not a simple function of Z but depends on the CO filling factor which can be partly recovered from the models (*Ramambason+ in prep.*)

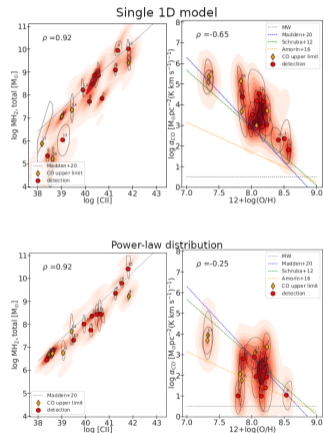
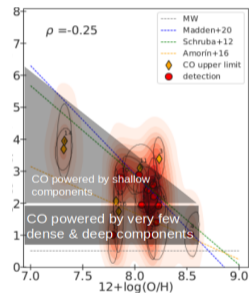
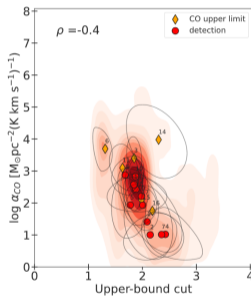
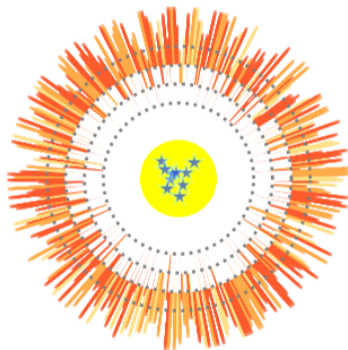


Fig.: CO-to-H<sub>2</sub> value between MW value and extreme case of CO uniformly distributed (*Ramambason+ in prep.*) ( $\Rightarrow$  **L. Ramambason's poster**)

## CO-dark



Possible to recover distributions of dense clouds even for integrated galaxies



# PDR heating

## Limits of the PE heating

- Evidence for PAH emission tracing (and PAH carriers likely dominating) neutral atomic gas heating through PE (*Helou+ 2001, Croxall+ 2012, Lebouteiller+ 2012, 2019, Lambert-Huyghe+ 2022, Berné+ 2022*)
- Low D/G and PAH abundance (*e.g., Galliano+ 2021*)  $\Rightarrow$  low Z? Compensation by very small grains? By other heating mechanisms related to SF?

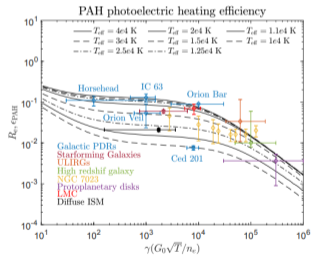


Fig.: PE heating efficiency and observational proxy  $(\text{CII})+(\text{OI}) / \text{PAH}$  (Berné+ 2022)

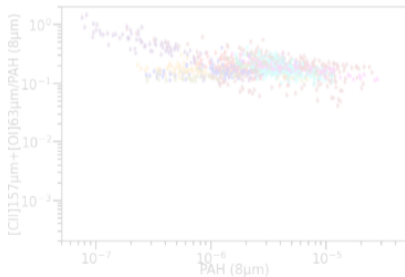


Fig.:  $(\text{CII})+(\text{OI}) / \text{PAH}$  in Magellanic Clouds (Lambert-Huyghe+ 2022)

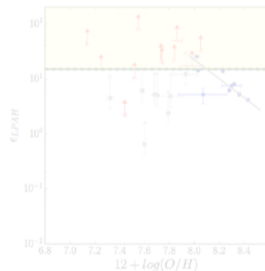


Fig.: PAH heating efficiency vs. Z (de la Vieuville+ unpublished)

# PDR heating

## Limits of the PE heating

- Evidence for PAH emission tracing (and PAH carriers likely dominating) neutral atomic gas heating through PE (*Helou+ 2001, Croxall+ 2012, Lebouteiller+ 2012, 2019, Lambert-Huyghe+ 2022, Berné+ 2022*)
- Low D/G and PAH abundance (*e.g., Galliano+ 2021*)  $\Rightarrow$  low Z? Compensation by very small grains? By other heating mechanisms related to SF?

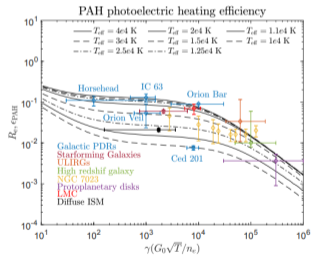


Fig.: PE heating efficiency and observational proxy  $(\text{CII})+(\text{OI}) / \text{PAH}$  (Berné+ 2022)

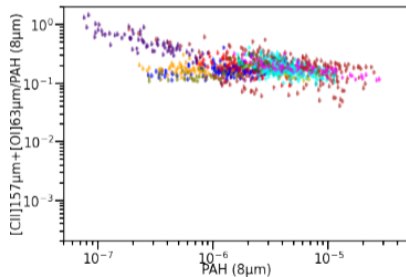


Fig.:  $(\text{CII})+(\text{OI}) / \text{PAH}$  in Magellanic Clouds (Lambert-Huyghe+ 2022)

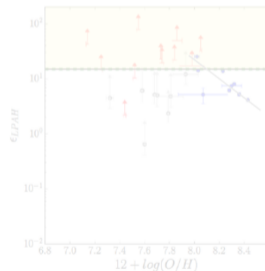
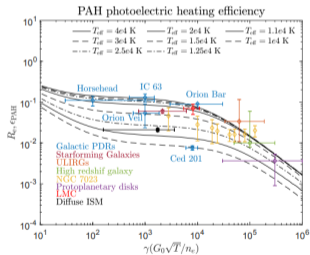


Fig.: PAH heating efficiency vs. Z (*de la Vieuville+ unpublished*)

# PDR heating

## Limits of the PE heating

- Evidence for PAH emission tracing (and PAH carriers likely dominating) neutral atomic gas heating through PE (*Helou+ 2001, Croxall+ 2012, Leboutellier+ 2012, 2019, Lambert-Huyghe+ 2022, Berné+ 2022*)
- Low D/G and PAH abundance (*e.g., Galliano+ 2021*)  $\Rightarrow$  low Z? Compensation by very small grains? By other heating mechanisms related to SF?



**Fig.:** PE heating efficiency and observational proxy  $(\text{CII})+(\text{OI}) / \text{PAH}$  (Berné+ 2022)

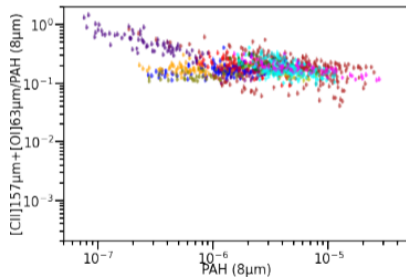


**Fig.:**  $(\text{CII})+(\text{OI}) / \text{PAH}$  in Magellanic Clouds (Lambert-Huyghe+ 2022)

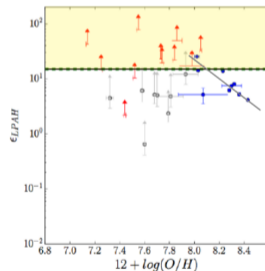


**Fig.:** PAH heating efficiency vs. Z (de la Vieville+ unpublished)

# Pushing (CII) and PE to the limit

## Model

- IZw18, 18Mpc,  $1/35 Z_{\odot}$ , D/G  $\sim 1000$  lower than MW

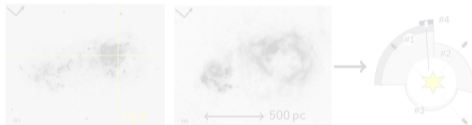


Fig.: IZw18 modeling strategy (Lebouteiller+ 2017)

## Beyond the MW PE paradigm

- Single ULX dominates neutral gas heating with negligible contribution from PE
- (CII) traces an almost purely neutral atomic gas

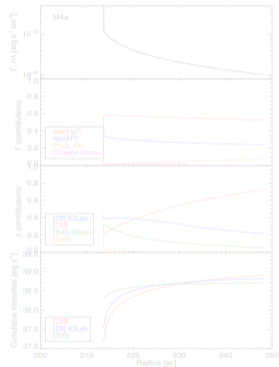


Fig.: Cooling/heating contributions in the radiation-bounded (PDR) sector (Lebouteiller+ 2017)

# Pushing (CII) and PE to the limit

## Model

- IZw18, 18Mpc,  $1/35 Z_{\odot}$ , D/G  $\sim 1000$  lower than MW

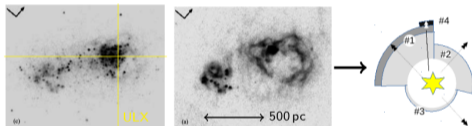


Fig.: IZw18 modeling strategy (Lebouteiller+ 2017)

## Beyond the MW PE paradigm

- Single ULX dominates neutral gas heating with negligible contribution from PE
- (CII) traces an almost purely neutral atomic gas

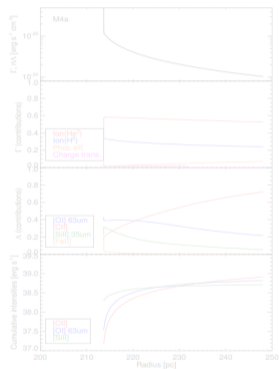


Fig.: Cooling/heating contributions in the radiation-bounded (PDR) sector (Lebouteiller+ 2017)

# Pushing (CII) and PE to the limit

## Model

- IZw18, 18Mpc,  $1/35 Z_{\odot}$ , D/G  $\sim 1000$  lower than MW

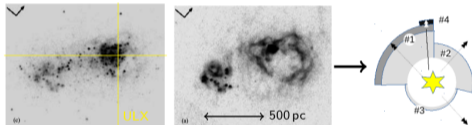


Fig.: IZw18 modeling strategy (Lebouteiller+ 2017)

## Beyond the MW PE paradigm

- Single ULX dominates neutral gas heating with negligible contribution from PE
- (CII) traces an almost purely neutral atomic gas

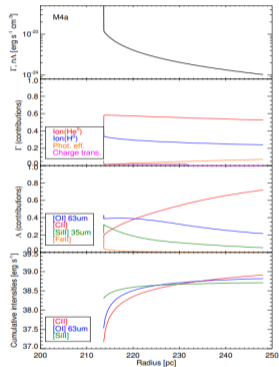


Fig.: Cooling/heating contributions in the radiation-bounded (PDR) sector (Lebouteiller+ 2017)

# Cosmic rays

## CRIR

- $\text{H}_3^+$  measurements:  $\zeta_H \approx 3 \times 10^{-16} \text{ s}^{-1}$  MW disk (e.g., Indriolo+ 2009, 2012),  $\sim 10 - 1000$  larger in GC (Oka+ 2019)
- Nearby SB galaxy disks (e.g., Van der Tak+ 2016), nuclei (e.g., ALCHEMI, Holdship+ 2022), and ULIRG nuclei (e.g., González-Alfonso+ 2018) with ionized molecules in dense gas (e.g.,  $\text{H}_2\text{O}^+$ ), even lensed galaxies beyond  $z > 2$  (Indriolo+ 2018), all suggesting MW-like range of values  $10^{-16}, -13 \text{ s}^{-1}$ .
- $\zeta_H$  is larger in regions of more copious star formation: depends on proximity to cosmic-ray accelerators, particle propagation effects, and losses via interactions with the ISM (Indriolo+ 2018)

## CR impact on ISM

- Ionization of molecules in dense gas  $\Rightarrow$  chemical network
- Along with gas density, CRIR impact ISM fractionation in external galaxies (isotopic ratios) (e.g. VIII+ 2019, 2020)
- Impacts the use of (CII) and (OI) through increased C,  $\text{C}^+$  column densities wrt CO, impacts somewhat  $X_{\text{CO}}$  factor as well (Bisbas+ 2021)
- Difficult distinction between CR and hard X-rays...

## Prospectives for the diffuse/large-scale ISM

- Cosmic-ray-induced near-IR  $\text{H}_2$  line emission with JWST (Bialy+ 2021, Gaches+ 2022)
- Also  $\text{H}_3^+$  with JWST (Indriolo+ 2007)

# Cosmic rays

## CRIR

- $\text{H}_3^+$  measurements:  $\zeta_H \approx 3 \times 10^{-16} \text{ s}^{-1}$  MW disk (e.g., Indriolo+ 2009, 2012),  $\sim 10 - 1000$  larger in GC (Oka+ 2019)
- Nearby SB galaxy disks (e.g., Van der Tak+ 2016), nuclei (e.g., ALCHEMI, Holdship+ 2022), and ULIRG nuclei (e.g., González-Alfonso+ 2018) with ionized molecules in dense gas (e.g.,  $\text{H}_2\text{O}^+$ ), even lensed galaxies beyond  $z > 2$  (Indriolo+ 2018), all suggesting MW-like range of values  $10^{-16}, -13 \text{ s}^{-1}$ .
- $\zeta_H$  is larger in regions of more copious star formation: depends on proximity to cosmic-ray accelerators, particle propagation effects, and losses via interactions with the ISM (Indriolo+ 2018)

## CR impact on ISM

- Ionization of molecules in dense gas  $\Rightarrow$  chemical network
- Along with gas density, CRIR impact ISM fractionation in external galaxies (isotopic ratios) (e.g., Viti+ 2019, 2020)
- Impacts the use of (CII) and (OI) through increased C,  $\text{C}^+$  column densities wrt CO, impacts somewhat  $X_{\text{CO}}$  factor as well (Bisbas+ 2021)
- Difficult distinction between CR and hard X-rays...

## Prospectives for the diffuse/large-scale ISM

- Cosmic-ray-induced near-IR  $\text{H}_2$  line emission with JWST (Bialy+ 2021, Gaches+ 2022)
- Also  $\text{H}_3^+$  with JWST (Indriolo+ 2007)



# Cosmic rays

## CRIR

- $\text{H}_3^+$  measurements:  $\zeta_H \approx 3 \times 10^{-16} \text{ s}^{-1}$  MW disk (e.g., Indriolo+ 2009, 2012),  $\sim 10 - 1000$  larger in GC (Oka+ 2019)
- Nearby SB galaxy disks (e.g., Van der Tak+ 2016), nuclei (e.g., ALCHEMI, Holdship+ 2022), and ULIRG nuclei (e.g., González-Alfonso+ 2018) with ionized molecules in dense gas (e.g.,  $\text{H}_2\text{O}^+$ ), even lensed galaxies beyond  $z > 2$  (Indriolo+ 2018), all suggesting MW-like range of values  $10^{-16}, -13 \text{ s}^{-1}$ .
- $\zeta_H$  is larger in regions of more copious star formation: depends on proximity to cosmic-ray accelerators, particle propagation effects, and losses via interactions with the ISM (Indriolo+ 2018)

## CR impact on ISM

- Ionization of molecules in dense gas  $\Rightarrow$  chemical network
- Along with gas density, CRIR impact ISM fractionation in external galaxies (isotopic ratios) (e.g., Viti+ 2019, 2020)
- Impacts the use of (CII) and (OI) through increased C,  $\text{C}^+$  column densities wrt CO, impacts somewhat  $X_{\text{CO}}$  factor as well (Bisbas+ 2021)
- Difficult distinction between CR and hard X-rays...

## Prospectives for the diffuse/large-scale ISM

- Cosmic-ray-induced near-IR  $\text{H}_2$  line emission with JWST (Bialy+ 2021, Gaches+ 2022)
- Also  $\text{H}_3^+$  with JWST (Indriolo+ 2007)

# Formation/destruction timescales of molecular clouds

- PHANGS-\* (ALMA, H $\alpha$ , MUSE, VLA...): timescales for GMC formation, cluster formation, HII region formation and front expansion, decorrelation cloud/cluster

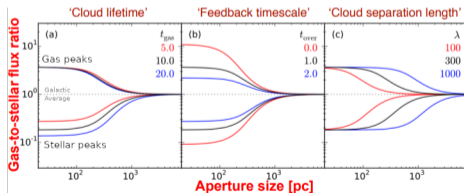
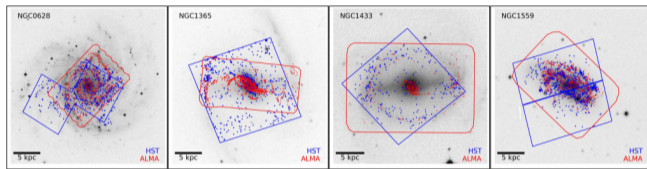


Fig.: Gas-to-SFR ratio, see, e.g., (Krujissen+ 2019, Chevance+ 2022a)

# Formation/destruction timescales of molecular clouds (cont'd)

## Short-lived molecular clouds and rapid feedback $\Rightarrow$ inefficient SF

### LMC

- LMC: GMC lifetime  $\approx 11$  Myr likely set by internal processes rather than galactic dynamics, **contrary to HI clouds** (Ward+ 2022)

### MS galaxies

- Molecular cloud lifetime ("inert" phase)  $\sim 16$  Myr (Kim+ 2022)
- Efficiently dispersed by stellar feedback within 1-5 Myr once the star-forming region becomes partially exposed. Early feedback mechanisms (photoionisation and stellar winds) efficiently disperse molecular clouds, prior to SNe explosions (see also Chevance+ 2022b)  $\Rightarrow$  **A. Zakardjian's talk**
- (integrated cloud-scale star formation efficiency  $\approx 1-8\%$ )
- 1/2 CO and H $\alpha$  is diffuse
- CO-visible cloud lifetimes become shorter with decreasing galaxy mass, attributed to CO-dark H $_2$  mass at low Z

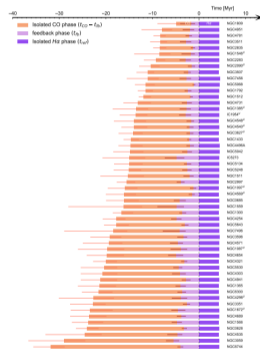
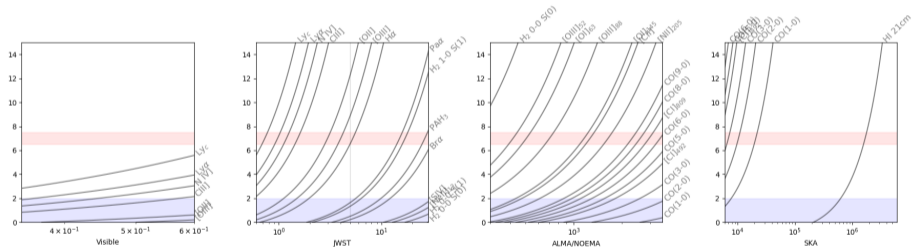


Fig.: Timescales for the various phases (Kim+ 2022).

# Last word on observations

Period is ripe for synergistic dataset analyses

- Resolved, IFUs: (Blue)MUSE, JWST, ALMA/NOEMA then SKA
- Sweet spot @  $z \lesssim 2$  (UV  $\rightarrow$  opt., opt.  $\rightarrow$  NIRspec, near-IR  $\rightarrow$  MIRI, CO ladder with ALMA)
- Sweet spot @  $z \sim 7$  (UV  $\rightarrow$  NIRspec, far-IR  $\rightarrow$  ALMA, CO  $\rightarrow$  SKA)



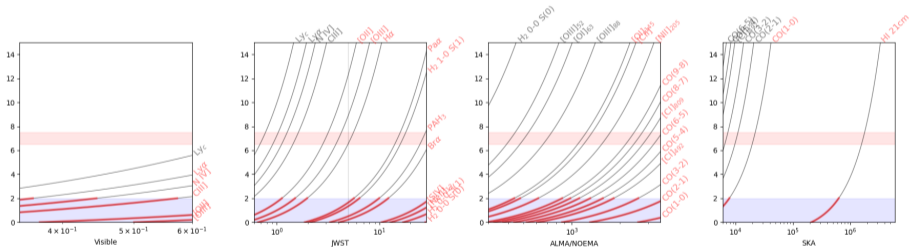
Few considerations

- UV emission lines N IV, C IV, He II, O III, Si III, C III)... ( $\sim 1400\text{-}1900\text{\AA}$ ): accurate diagnostics for E(B-V),  $n_e$ ,  $T_e$ , O/H, U... (Mingozzi+ 2022)
- Mid-IR diagnostics will remain unavailable at  $z \sim 2 - 10$  until PRIMA (<http://agora.lam.fr>)

# Last word on observations

Period is ripe for synergistic dataset analyses

- Resolved, IFUs: (Blue)MUSE, JWST, ALMA/NOEMA then SKA
- Sweet spot @  $z \lesssim 2$  (UV  $\rightarrow$  opt., opt.  $\rightarrow$  NIRspec, near-IR  $\rightarrow$  MIRI, CO ladder with ALMA)
- Sweet spot @  $z \sim 7$  (UV  $\rightarrow$  NIRspec, far-IR  $\rightarrow$  ALMA, CO  $\rightarrow$  SKA)



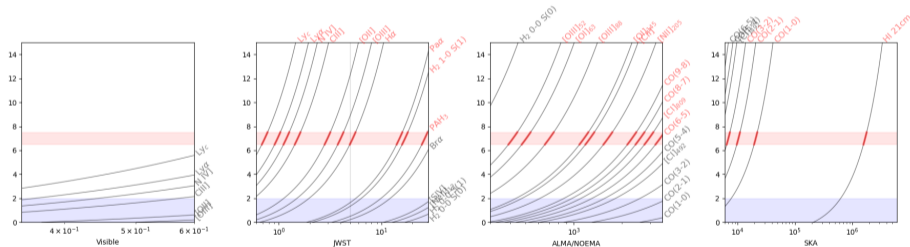
Few considerations

- UV emission lines N IV, C IV, He II, O III, Si III, C III)... (~1400-1900Å): accurate diagnostics for E(B-V),  $n_e$ ,  $T_e$ , O/H, U... (Mingozzi+ 2022)
- Mid-IR diagnostics will remain unavailable at  $z \sim 2 - 10$  until PRIMA (<http://agora.lam.fr>)

# Last word on observations

Period is ripe for synergistic dataset analyses

- Resolved, IFUs: (Blue)MUSE, JWST, ALMA/NOEMA then SKA
- Sweet spot @  $z \lesssim 2$  (UV  $\rightarrow$  opt., opt.  $\rightarrow$  NIRspec, near-IR  $\rightarrow$  MIRI, CO ladder with ALMA)
- Sweet spot @  $z \sim 7$  (UV  $\rightarrow$  NIRspec, far-IR  $\rightarrow$  ALMA, CO  $\rightarrow$  SKA)



Few considerations

- UV emission lines N IV, C IV, He II, O III, Si III, C III)... ( $\sim 1400\text{-}1900\text{\AA}$ ): accurate diagnostics for E(B-V),  $n_e$ ,  $T_e$ , O/H, U... (Mingozzi+ 2022)
- Mid-IR diagnostics will remain unavailable at  $z \sim 2 - 10$  until PRIMA (<http://agora.lam.fr>)

# Modeling strategies

# Scale & adapt

## Challenges

- Integrate **adapted prescriptions** in models (e.g., low metallicity chemistry, dust properties etc. . . ) and in the **input energetic sources**
- Distinguish **physical processes** for galaxies (e.g., photoionization, shocks, turbulence, B, CRs. . . ) from spatially/spectrally unresolved tracers
- Account for **ISM complexity** (e.g., phases, distribution of matter. . . )
- Account for **geometry** gas+sources (distribution, optical depth, projection effects. . . ), only partly alleviated by spatial/spectral decomposition and/or IFUs
- High level of degeneracy  $\Rightarrow$  manage **multiple solutions** in large grids



# Many potential approaches

Method	Advantages	Difficulties
Simulations	Dynamical effects, large volume 3D RT post-processing tools exist, e.g., with MOCASSIN	Comparison with specific observations (statistics), light chemistry network
1D	State-of-the-art RT & chemistry	Scale to complex geometries
Pure 3D	3D RT, diffuse light. . .	Geometry (gas+sources) not free parameter
MC 3D	Good 3D approximation	Geometry not free parameter
Pseudo-3D from 1D	State-of-the-art RT & chemistry Central ionizing source (AGN, PN, HII region)	Not 3D! Geometry not free parameter
Topological 3D from 1D	Inferred geometry	Not 3D!

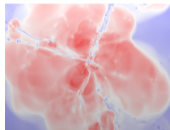


Fig.: SPHINX (Rosdhal+ 2018)



Fig.: MOCASSIN (Hubber+ 2016)



Fig.: M3-MAPPINGS V (Jin+ 2022)



Fig.: M3-MAPPINGS V (Jin+ 2022)



Fig.: PyCloudy, PyCROSS (Fitzgerald+ 2020; Morisset+ 2013)



Fig.: MULTIGRIS+Cloudy (Lebouteiller Ramambason 2022)

# Many potential approaches

Method	Advantages	Difficulties
Simulations	Dynamical effects, large volume 3D RT post-processing tools exist, e.g., with MOCASSIN	Comparison with specific observations (statistics), light chemistry network
1D	State-of-the-art RT & chemistry	Scale to complex geometries
Pure 3D	3D RT, diffuse light. . .	Geometry (gas+sources) not free parameter
MC 3D	Good 3D approximation	Geometry not free parameter
Pseudo-3D from 1D	State-of-the-art RT & chemistry	Not 3D! Geometry not free parameter
Topological 3D from 1D	Central ionizing source (AGN, PN, HII region) Inferred geometry	Not 3D!

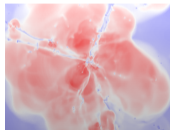


Fig.: SPHINX (Rosdhal+ 2018)



Fig.: MOCASSIN (Hubber+ 2016)



Fig.: M3-MAPPINGS V (Jin+ 2022)



Fig.: M3-MAPPINGS V (Jin+ 2022)



Fig.: PyCloudy, PyCROSS (Fitzgerald+ 2020; Morisset+ 2013)



Fig.: MULTIGRIS+Cloudy (Leboutellier Ramambason 2022)

# Many potential approaches

Method	Advantages	Difficulties
Simulations	Dynamical effects, large volume 3D RT post-processing tools exist, e.g., with MOCASSIN	Comparison with specific observations (statistics), light chemistry network
1D	State-of-the-art RT & chemistry	Scale to complex geometries
Pure 3D	3D RT, diffuse light. . .	Geometry (gas+sources) not free parameter
MC 3D	Good 3D approximation	Geometry not free parameter
Pseudo-3D from 1D	State-of-the-art RT & chemistry	Not 3D! Geometry not free parameter
Topological 3D from 1D	Central ionizing source (AGN, PN, HII region) Inferred geometry	Not 3D!

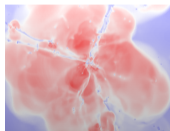


Fig.: SPHINX (Rosdhal+ 2018)

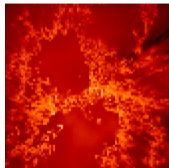


Fig.: MOCASSIN (Hubber+ 2016)



Fig.: M3-MAPPINGS V (Jin+ 2022)



Fig.: M3-MAPPINGS V (Jin+ 2022)



Fig.: PyCloudy, PyCROSS (Fitzgerald+ 2020; Morisset+ 2013)



Fig.: MULTIGRIS+Cloudy (Lebouteiller Ramambason 2022)

# Many potential approaches

Method	Advantages	Difficulties
Simulations	Dynamical effects, large volume 3D RT post-processing tools exist, e.g., with MOCASSIN	Comparison with specific observations (statistics), light chemistry network
1D	State-of-the-art RT & chemistry	Scale to complex geometries
Pure 3D	3D RT, diffuse light. . .	Geometry (gas+sources) not free parameter
MC 3D	Good 3D approximation	Geometry not free parameter
Pseudo-3D from 1D	State-of-the-art RT & chemistry Central ionizing source (AGN, PN, HII region)	Not 3D! Geometry not free parameter
Topological 3D from 1D	Inferred geometry	Not 3D!

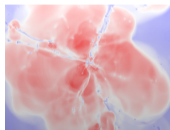


Fig.: SPHINX (Rosdhal+ 2018)

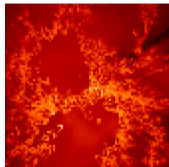


Fig.: MOCASSIN (Hubber+ 2016)

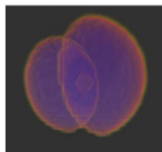


Fig.: M3-MAPPINGS V (Jin+ 2022)

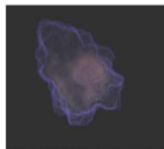


Fig.: M3-MAPPINGS V (Jin+ 2022)



Fig.: PyCloudy, PyCROSS (Fitzgerald+ 2020; Morisset+ 2013)



Fig.: MULTIGRIS+Cloudy (Lebouteiller Ramambason 2022)

# Many potential approaches

Method	Advantages	Difficulties
Simulations	Dynamical effects, large volume 3D RT post-processing tools exist, e.g., with MOCASSIN	Comparison with specific observations (statistics), light chemistry network
1D	State-of-the-art RT & chemistry	Scale to complex geometries
Pure 3D	3D RT, diffuse light. . .	Geometry (gas+sources) not free parameter
MC 3D	Good 3D approximation	Geometry not free parameter
Pseudo-3D from 1D	State-of-the-art RT & chemistry Central ionizing source (AGN, PN, HII region)	Not 3D! Geometry not free parameter
Topological 3D from 1D	Inferred geometry	Not 3D!

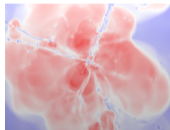


Fig.: SPHINX (Rosdhal+ 2018)

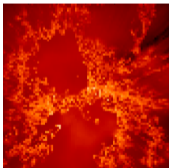


Fig.: MOCASSIN (Hubber+ 2016)

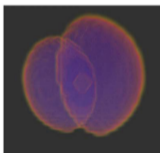


Fig.: M3-MAPPINGS V (Jin+ 2022)

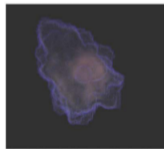


Fig.: M3-MAPPINGS V (Jin+ 2022)

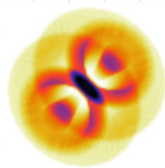


Fig.: PyCloudy, PyCROSS  
(Fitzgerald+ 2020; Morisset+ 2013)



Fig.: MULTIGRIS+Cloudy  
(Lebouteiller Ramambason 2022)

# Many potential approaches

Method	Advantages	Difficulties
Simulations	Dynamical effects, large volume 3D RT post-processing tools exist, e.g., with MOCASSIN	Comparison with specific observations (statistics), light chemistry network
1D	State-of-the-art RT & chemistry	Scale to complex geometries
Pure 3D	3D RT, diffuse light. . .	Geometry (gas+sources) not free parameter
MC 3D	Good 3D approximation	Geometry not free parameter
Pseudo-3D from 1D	State-of-the-art RT & chemistry Central ionizing source (AGN, PN, HII region)	Not 3D! Geometry not free parameter
Topological 3D from 1D	Inferred geometry	Not 3D!

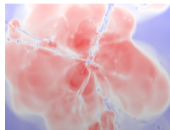


Fig.: SPHINX (Rosdhal+ 2018)

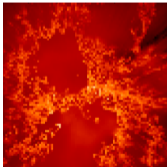


Fig.: MOCASSIN (Hubber+ 2016)

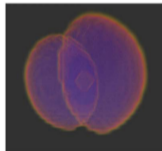


Fig.: M3-MAPPINGS V (Jin+ 2022)

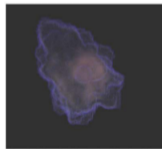


Fig.: M3-MAPPINGS V (Jin+ 2022)

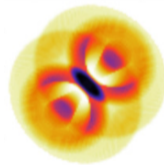


Fig.: PyCloudy, PyCROSS  
(Fitzgerald+ 2020; Morisset+ 2013)

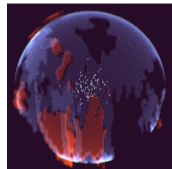
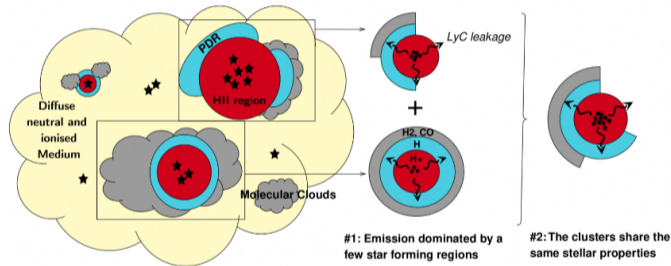


Fig.: MULTIGRIS+Cloudy  
(Lebouteiller Ramambason 2022)

# Topological models: multi-sector

- Observed emission is the sum of N components distributed in several stellar clusters surrounded with several sectors described by 1D models  
(Péquignot 2008, Cormier+ 2012, Cormier+ 2019, Leboutellier+ 2017, Polles+ 2019, Leboutellier Ramambason 2022, Ramambason+ 2022)

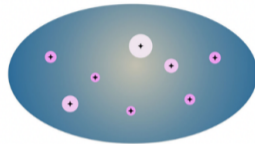
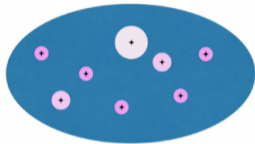
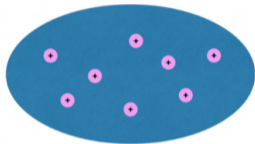


## Explanations

- Combine 1D models that propagate radiation through HII region+PDR(+molecular cloud)  $\Rightarrow$  1D (depth) structure constrained, need to constrain the spherical geometry (diffuse/reflected light and geometry simplification but still better than 1D though...!)

# Topological models: locally optimally emitting clouds (LOC)

- Observed emission is the result of strong selection effects due to the fact that some lines emit preferentially under some physical conditions (Ferguson+ 1997, Richardson+ 2014, 2016).



$$L_{line} = \underbrace{\int \dots \int}_n L(p_1, \dots, p_n) \psi(p_1, \dots, p_n) dp_1 \dots dp_n$$

$$\psi = U^\alpha U n^{\alpha_n} \dots$$

## Applications

- Machine Learning application (Morisset+ in prep.)
- Depth/ $A_V$ : Application to statistical distribution of clouds with log-normal  $A_V$  in PDRs (Bisbas+ 2019)
  - + power-law tail due to self-gravity (possibly leading to star formation) reminiscent of result obtained in Ramambason+ (2022) for which only power-law distributions of depth can reproduce CO emission.



# Global SED approach adapted to galaxy evolution parameters ( $z$ , SFH, IMF...)

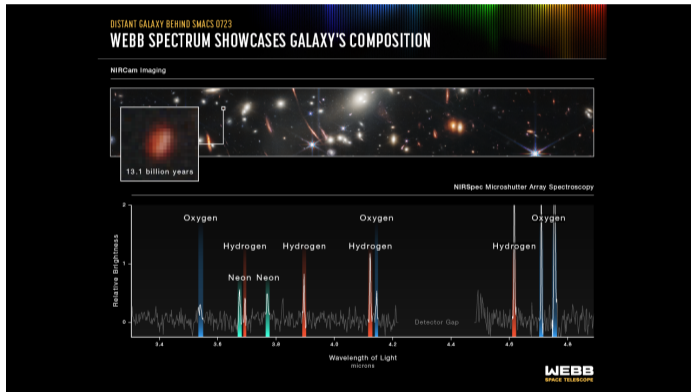
## Galaxy-wide parameters & gas properties

- CIGALE & x-CIGALE: global energy balance (Boquiou+ 2019)
  - Full SED models from far-UV to far-IR
  - Using geometry templates for dust attenuation
- BEAGLE (Chevallard Charlot 2016)
  - Dust attenuation prescription related to inclination, global geometry (e.g., disk, bulge)
  - RT through ISM & IGM
- **General**
  - Nebular emission is accounted for (PDRs and CO in progress)
  - So far simple grids with tabulated  $U$  and  $Z$ , constant  $n \sim 100 \text{ cm}^{-3}$



# Complex models for single spectra

Still a relevant problem for single-dish/long-wavelength observations or for distant Universe



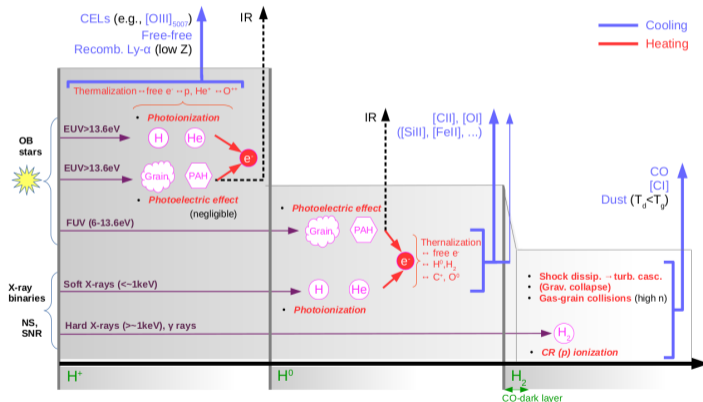
Objective: use the tracers to recover model parameters, including potentially geometry

End

# Physical processes to explore in a comprehensive way (cont'd)

## Energy input and gas heating mechanisms

- **Neutral atomic gas:** PE heating, soft X-rays, CRs...
- **Molecular gas:** hard X-rays, shocks, cosmic ray ionization...
- Main challenge: knowledge on dust content, X-ray sources, CR propagation and SFR dependency
- **All phases/scales:** shocks expected from various sources acting on various scales (from mergers, AGNs, starbursts... to protostellar outflows and stellar winds)
- Main challenge: lack of spatial decomposition/resolution – mixing biases



# Dense gas fractions and SFE

## Dense gas fraction in extragalactic ISM

- HCN, HCO<sup>+</sup> more and more observations but still few studies apart from very nearby galaxies (e.g., Magellanic Clouds; *Galamez+ 2020*) and starbursts/AGNs
- Consistent results in that SFE  $\searrow$  when dense gas fraction (or stellar surface density, interstellar P...)  $\nearrow$ , at kpc-scales (*EMPIRE; Jiménez-Donaire+ 2019*) down to <100pc-scales (*Beslic+ 2021, PAWS Schinnerer in prep.*)
- SFE traced by IR/HCN or H $\alpha$ /HCN

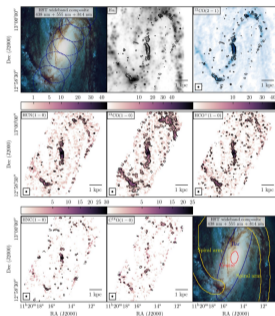


Fig.: NGC3627 with NOEMA and PHANGS-MUSE (Beslic+ 2021)

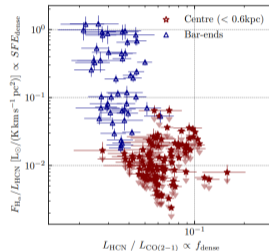


Fig.: SFE(dense) vs. f(dense) in NGC3627 (Beslic+ 2021)

All in all favoring turbulence-regulated SF models (e.g., Burkharth & Mocz 2018)

# & much more...

## Shocks

- Near/mid-IR  $H_2$  as well as optical lines for tracing relatively diffuse shocks (e.g., Hong+ 2013, Medling+ 2015) but difficult interpretation without spatial resolution JWST important for nearby galaxies

## Dust and mineralogy with JWST

- PAHs, fullerenes,  $CO_2$  ice...
- Spitzer: crystalline silicates are a common component of the ISM (Spoon+ 2022)
- Strength of crystalline silicate bands toward nuclei correlate with strength of amorphous silicate strength
- Transition from emission to absorption at high obscuration consistent with an origin for the amorphous/crystalline silicate features in a centrally heated dust geometry (edge-on disk or cocoon).
- Crystalline silicate bands able to classify the obscuration level of AGNs, even in the presence of strong circumnuclear star formation

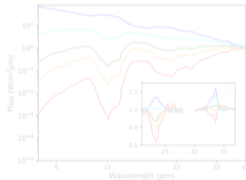


Fig.: Simulated MIR spectra of centrally heated dust shells with increasing dust mass (Spoon+ 2022) – amorphous silicates.

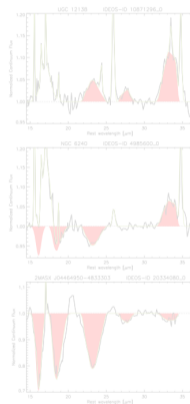


Fig.: Observed spectra showing the transition emission/absorption for crystalline silicates (Spoon+ 2022).

# & much more...

## Shocks

- Near/mid-IR H<sub>2</sub> as well as optical lines for tracing relatively diffuse shocks (e.g., Hong+ 2013, Medling+ 2015) but difficult interpretation without spatial resolution JWST important for nearby galaxies

## Dust and mineralogy with JWST

- PAHs, fullerenes, CO<sub>2</sub> ice...
- Spitzer: crystalline silicates are a common component of the ISM (Spoon+ 2022)
- Strength of crystalline silicate bands toward nuclei correlate with strength of amorphous silicate strength
- Transition from emission to absorption at high obscuration consistent with an origin for the amorphous/crystalline silicate features in a centrally heated dust geometry (edge-on disk or cocoon).
- Crystalline silicate bands able to classify the obscuration level of AGNs, even in the presence of strong circumnuclear star formation

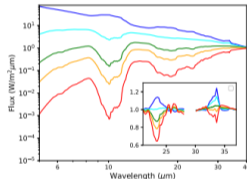


Fig.: Simulated MIR spectra of centrally heated dust shells with increasing dust mass (Spoon+ 2022) – amorphous silicates.

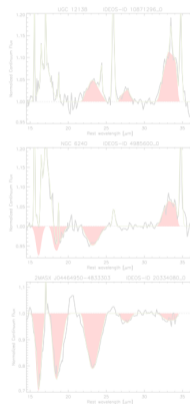


Fig.: Observed spectra showing the transition emission/absorption for crystalline silicates (Spoon+ 2022).

# & much more...

## Shocks

- Near/mid-IR H<sub>2</sub> as well as optical lines for tracing relatively diffuse shocks (e.g., Hong+ 2013, Medling+ 2015) but difficult interpretation without spatial resolution JWST important for nearby galaxies

## Dust and mineralogy with JWST

- PAHs, fullerenes, CO<sub>2</sub> ice...
- Spitzer: crystalline silicates are a common component of the ISM (Spoon+ 2022)
- Strength of crystalline silicate bands toward nuclei correlate with strength of amorphous silicate strength
- Transition from emission to absorption at high obscuration consistent with an origin for the amorphous/crystalline silicate features in a centrally heated dust geometry (edge-on disk or cocoon).
- Crystalline silicate bands able to classify the obscuration level of AGNs, even in the presence of strong circumnuclear star formation

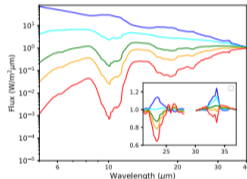


Fig.: Simulated MIR spectra of centrally heated dust shells with increasing dust mass (Spoon+ 2022) – amorphous silicates.

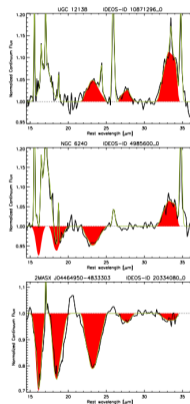


Fig.: Observed spectra showing the transition emission/absorption for crystalline silicates (Spoon+ 2022).